









Middle Devonian reef-derived calciturbidites of western Ossa-Morena Zone (Portugal): conodont biostratigraphy of the Eifelian Pedreira da Engenharia Limestone

Gonçalo Silvério^{1,2}  · Jau-Chyn Liao³  · José I. Valenzuela-Ríos⁴  · Gil Machado^{5,6}  · Pedro Barreto⁷  · Noel Moreira^{1,2} 

Received: 1 November 2023 / Accepted: 28 May 2024

© The Author(s) 2024

Abstract

The first biostratigraphical study on the complete Pedreira da Engenharia quarry section (Middle Devonian, SW Portugal) is presented. A total of 32 samples were collected from the three subsections (PE-A, quarry floor; PE-B and PE-C). This led to the identification of 15 species belonging to the genera *Icriodus*, *Polygnathus* and *Tortodus*. Four index species were identified: *P. costatus*; *T. australis*; *T. kockelianus*; and *P. ensensis*. The age for the Pedreira da Engenharia section was updated from the *costatus* zone (Boogaard, 1972) to the *costatus-ensensis* zones (lower to uppermost Eifelian). There is a thin part of the succession representing the *kockelianus* and, possibly, *eiflius* zones, together being represented by 1,5 m. A CAI value of 5-5.5 for the conodont elements indicates a maximum temperature of over 300 °C. The Pedreira da Engenharia Limestone, together with the Odivelas Limestone, are evidence of the development of calciturbidite sedimentation associated with atoll-like structures (only preserved in Odivelas) along the SW boundary of Ossa-Morena Zone, being probably associated with the beginning of the subduction of the Rheic Ocean during Early to Middle Devonian times.

Keywords Eifelian · Conodonts · Calciturbidites · Pedreira da Engenharia limestone · Cabrela Basin · Ossa-Morena Zone

Resumen

Se presenta el primer estudio bioestratigráfico completo de la sección de la cantera de Pedreira da Engenharia (Devónico Medio, SO de Portugal). Un total de 32 muestras fueron colectadas de las tres secciones (PE-A, la base de la cantera; PE-B y PE-C). Esto llevó a la identificación de 15 especies pertenecientes a los géneros *Icriodus*, *Polygnathus* y *Tortodus*. Se identificaron cuatro especies índice: *P. costatus*; *T. australis*; *T. kockelianus*; y *P. ensensis*. La edad de la sección Pedreira da Engenharia se actualizó desde la zona *costatus* (Boogaard, 1972) a las zonas *costatus-ensensis* (Eifeliense inferior a superior). La biozona *kockelianus*, y posiblemente la biozona *eiflius*, se encuentra representada en la sucesión por un reducido espesor de 1,5 m. Un valor CAI de 5-5,5 para los elementos conodontales indica una temperatura máxima superior a 300 °C. Las Calizas de Pedreira da Engenharia, junto con las Calizas de Odivelas, son evidencia del desarrollo de sedimentación calciturbidítica asociada a estructuras tipo atol (sólo preservadas en Odivelas) a lo largo del límite SO de la Zona de Ossa-Morena, probablemente asociadas con el inicio de la subducción del Océano Rheic durante el Devónico Inferior a Medio.

✉ Gonçalo Silvério
gsilverio@uevora.pt

¹ Instituto de Ciências da Terra, Polo-Évora, Rua Romão Ramalho 59, 7000-671 Évora, Portugal

² Instituto de Investigação e Formação Avançada, University of Evora, Palácio do Vimioso, Largo Marquês de Marialva, Apart. 94, 7002-554 Évora, Portugal

³ Department of Geodynamic, Stratigraphy and Paleontology, University Complutense of Madrid, c/ José Antonio Novais 12, 28040 Madrid, Spain

⁴ Department of Botany and Geology, University of Valencia, C/Dr. Moliner 50, 46100 Burjassot, Spain

⁵ Chronosurveys, Av. 25 Abril n7 17dto., 2800-300 Almada, Portugal

⁶ Instituto Dom Luiz, University of Lisbon, Campo Grande C6, 1749-016 Lisboa, Portugal

⁷ Geo Logica, Rua de Colaride, 8, R/C E, 2735-208 Agualva, Portugal

Palabras clave Eifeliense · Conodontos · Calciturbiditas · Calizas de Pradeira da Engenharia · Cuenca de Cabrela · Zona Ossa-Morena

1 Introduction

Conodont studies on the Portuguese domain of the Ossa-Morena Zone (OMZ) are rare, mostly lack biostratigraphical detail and mainly focus on determining the age of particular limestone outcrops (e.g.: Boogaard, 1972, 1983; Piçarra & Sarmiento, 2006; Sarmiento et al., 2000, 2008, 2011). These studies evidenced a Devonian age of some limestone outcrops along the southwest boundary of the OMZ, but a detailed conodont-based biostratigraphical analysis is missing.

Recent studies on the Odivelas Limestone (Fig. 1a; Machado et al., 2009, 2010, 2020a) have provided a detailed, conodont-based, biostratigraphy, recognizing the existence of carbonate sedimentation during the Early to Middle Devonian in the OMZ. However, other important Devonian

limestone units, such as the Pedreira da Engenharia (PE) and Atalaia limestones, outcropping in the westernmost part of the OMZ, have not been studied in detail.

Boogaard (1972) carried out the first study of conodonts in the PE section, focusing his work on the base of the quarry, which was active at the time. The samples he analyzed yielded conodont elements attributed to the *costatus* zone, which indicated a Couvinian age (a term formerly referring to the latest Emsian to earliest Givetian; Bultynck, 2006).

Since that work, the Eifelian conodont biostratigraphy has been greatly improved (e.g., Belka et al., 1997). The aim of this study is to expand the sampling record of the PE section into the quarry face, as well as to review the results of Boogaard (1972) for the base of the quarry.

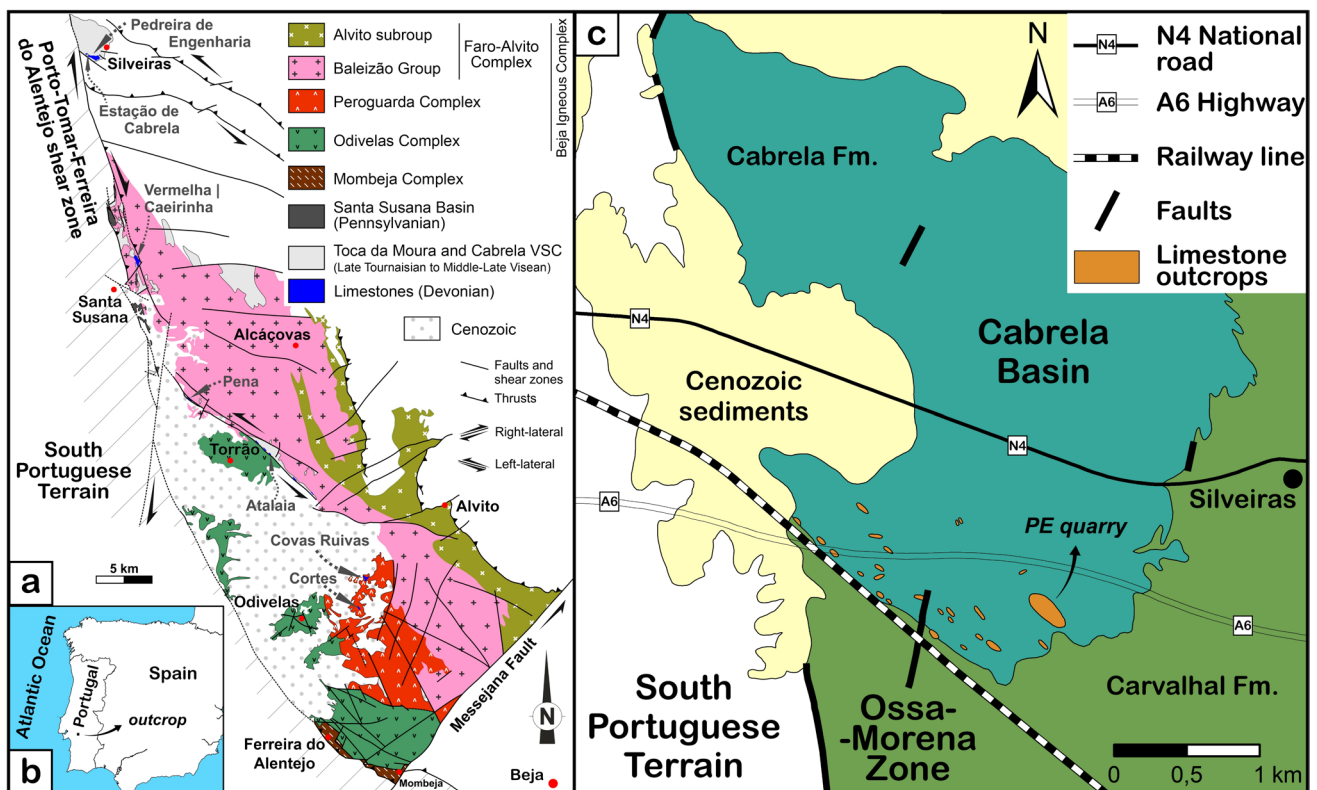


Fig. 1 Geographic and geological setting of the Pedreira da Engenharia Limestone. **a** Geologic map of the southwestern margin of the Ossa-Morena Zone, emphasizing the location of the main limestone occurrences (Pedreira da Engenharia, Estação de Cabrela, Caeirinha, Pena, Atalaia, Cortes and Covas Ruivas) (adapted from Andrade

et al., 1976; Machado et al., 2020b; Oliveira et al., 2019; Santos et al., 1990). **b** Geographic setting within the Iberian Peninsula. **c** Geologic map of the Cabrela Basin, with main roads and railroad. Geological basemap adapted from Carvalhosa and Zbyszewski (1994)

2 Geological setting

The PE quarry is located near the village of Silveiras (Montemor-o-Novo, Portugal; Fig. 1), within the Carboniferous Cabrela Basin, situated in a NW–SE oriented syncline close to the western limit of the OMZ, where it contacts with the South Portuguese Terrain (SPT) along the Porto-Tomar-Ferreira do Alentejo dextral shear zone (Fig. 1a; Carvalhosa & Zbyszewski, 1994; Moreira et al., 2014; Oliveira et al., 2013; Ribeiro et al., 2007).

2.1 Context within the Cabrela Basin

The PE Limestone and the Cabrela Formation (a Mississippian volcano-sedimentary unit composed of a siliciclastic turbiditic sequence with sparse carbonate lenses) constitute the Cabrela Basin succession (Oliveira et al., 1991, 2013, 2019), overlying the Carvalhal Formation, a volcano-sedimentary sequence of probable early to middle Cambrian age (Carvalhosa & Zbyszewski, 1994; Chichorro, 2006; Chichorro et al., 2008). The Carvalhal Formation is highly deformed and metamorphosed to phyllite and greenschist mafic rock facies (Carvalhosa & Zbyszewski, 1994; Chichorro et al., 2008; Ribeiro, 1983). The boundary between the Carvalhal and Cabrela formations is an unconformity and the two units differ in their tectono-metamorphic conditions (Oliveira et al., 2013, 2019; Pereira et al., 2006; Ribeiro, 1983). This unconformity is outlined by a polygenic conglomerate, containing boulders of greenschist facies lithotypes from the Carvalhal Formation, among other lithologies traceable to older OMZ units (Carvalhosa & Zbyszewski, 1994; Oliveira et al., 1991; Ribeiro, 1983). According to Ribeiro (1983), this polygenic conglomerate also overlies the PE Limestone, while the boundary between this limestone and the underlying Carvalhal Formation is marked by another polygenic conglomerate with lenticular shape, demarking an older unconformity (Oliveira et al., 1991; Ribeiro, 1983). The PE Limestone is Middle Devonian in age (Boogaard, 1972), being interpreted as distal deposits of turbidity currents composed of material derived from a local reef area, which is now eroded, or not outcropping (Jorge et al., 2018; Machado et al., 2020b; Moreira et al., 2021; Oliveira et al., 2019; Ribeiro, 1983).

Other limestone occurrences, similar to those reported in the PE quarry, including reefal, peri-reefal deposits and calciturbidites, have been described along the western boundary of OMZ (Machado et al., 2020b; Oliveira et al., 2019). These limestones date from the *patulus* (uppermost Emsian, Lower Devonian) to *hemiansatus* (lowermost Givetian, Middle Devonian) conodont zones (Machado & Hladil, 2010; Machado et al., 2009, 2010, 2020a; Oliveira et al., 2019) and suggest an alignment of atoll-like reef structures developed

along the southern border of the OMZ, during the Emsian to Givetian (Machado et al., 2020b; Moreira et al., 2021; Oliveira et al., 2019). Within the Cabrela Basin, limestones containing conodonts attributed to the lower *gigas* zone (currently lower *rhenana*) (upper Frasnian, Upper Devonian; Boogaard, 1983) have also been reported. However, their stratigraphical relation with other Devonian limestones and with the Cabrela Formation is not clear, preventing clear interpretations of their paleogeographic and geodynamic significance (Machado et al., 2020b).

2.2 The Pedreira da Engenharia Limestone: stratigraphy and structural features

The PE Limestone comprise a succession of dark-grey calciturbidites, with occasional dolostones, from the secondary dolomitization of the primary limestones (Moreira et al., 2019), interbedded with black shales (Jorge et al., 2018; Ribeiro, 1983). The grain size of the centimetric to decametric turbidite beds varies from fine sand, at the base, to clay, at the top (Jorge et al., 2018). This calciturbidite sequence has an approximate exposed thickness of 50 m. The first 20 m are mostly covered by debris from the quarry face and frequently submerged under the quarry pond, being only accessible during periods of severe drought (Fig. 2). Consequently, the assessment of the base of the PE sequence and the recognition of its relation with the bottom unit is often difficult.

The deformation in the PE Limestone differs from the one recognized in the Cabrela Formation, both in intensity and geometry of the folds (Theias et al., 2018). While the succession of the Cabrela Formation shows gentle to open symmetrical folds, with NW–SE vertical axial planes and slightly dipping hinge lines, the PE Limestone has cylindrical and closed, asymmetrical folds, locally with short, inverted limbs and axial planes dipping 80 °NE, although most of the succession has a monoclinical structure dipping 50 °NE (Fig. 2, Theias et al., 2018). This suggests a different tectonic history for the PE limestones and is in accordance with the described unconformity between the PE limestones and the Cabrela Formation (Oliveira et al., 1991; Ribeiro, 1983).

3 Material and methods

The ephemeral outcropping of the quarry floor (usually covered by water), together with the difficulty in accessing its northern face, led to a division of the section into three sequences, named PE-A, PE-B and PE-C (Fig. 2).

PE-A comprises the sequence between the first and last recognizable layers at the quarry floor. Sampling was restricted due to pond sediments and vegetation (Fig. 2).

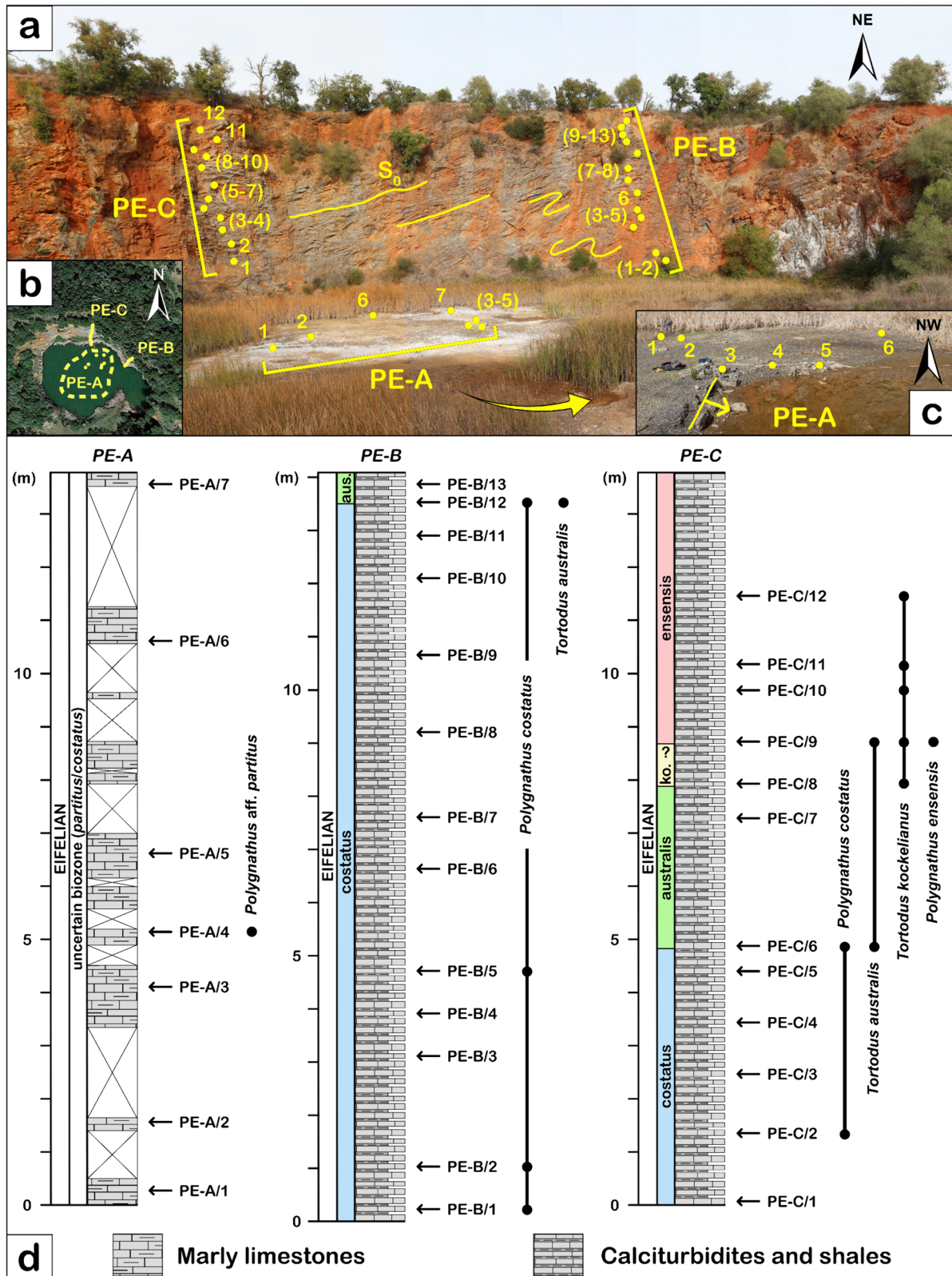


Fig. 2 Stratigraphic column of the Pedreira da Engenharia section. **a** Panoramic view of the quarry, with sampled areas marked in yellow and numbered according to their respective section. **b** Satellite image of the PE quarry showing the sampled sections. Satellite image is courtesy of Google Earth™. **c** Detailed view of the PE-A section

facings the orientation of the strata. **d** Stratigraphy of the PE section, indicating the sample levels and biostratigraphical data of the index conodont species and respective conodont zones marked in different colors

PE-B constitutes the middle part of the section, and is located on the NE face of the quarry, while PE-C corresponds to the third part of the section, located on the northern quarry face.

Due to the steepness and height of the quarry face (close to 20 m), sections PE-B and PE-C were sampled while abseiling. In these sections, samples were taken every 1 to 2 m, from the base of the calciturbidite beds, where the grain size is the coarsest, and close to the average size of conodonts. A total of 32 samples were collected in the quarry, 7 from PE-A, 13 from PE-B and 12 from PE-C (Fig. 2), each weighing 3 to 5 kg.

The samples were processed using formic acid ($\approx 8\%$) in 10 L solutions, suspended within the solution with the use of nets, allowing the smaller grains to fall to the bottom and the larger ones to maintain a large contact surface with the solution to improve the efficiency of the reaction. Once the reaction was complete, the samples were sieved at 1,5 mm mesh size, returning the larger particles to the acid solution for further reaction, and retaining the smaller particles in a separate bucket. The residue was then sorted through decantation, by adding water to the bucket, letting the water settle, and then eliminating unwanted particles in suspension, while maintaining the larger and/or heavier grains at the bottom.

The final residue was dried at a temperature no higher than 40 °C, in order to maintain the original coloration of the fossils. It was then sorted manually (under the microscope) or with the use of heavy liquids; bromoform, at an initial stage, and sodium polytungstate (SPT) at a later stage. Selected specimens were photographed using a scanning electron microscope (Hitachi S4800) at the University of Valencia (Spain).

4 Micropaleontology

4.1 General results

The fossils recovered from the residues are either phosphatic (conodonts), originally siliceous (sponge spicules) or silicified after deposition (dacryoconarids, bryozoans, ostracods and crinoids). All present a high level of fracturing and recementation (see Fig. 3p), especially the conodonts.

There is a significant difference between the paleontological content of samples from the PE-A section and those of the other two sections. With the exception of sample PE-A/4, all PE-A samples are barren of conodonts and dacryoconarids, but contain a significant amount of millimetric fragments of crinoids, visible with the naked eye, common fossils of uncertain origin (Fig. 3a–c), foraminifera and possible crustaceans (Fig. 3d). Samples from sections PE-B and PE-C, on the other hand, are dominated by dacryoconarids and conodonts.

In sections PE-B and PE-C, conodonts are present in a mean proportion of 25 elements/kg of sample. Most are fractured S elements, not suitable for specific identification. All elements present a black color, with a CAI index of 5–5.5. In the case of sponge spicules and bryozoans, the proportions are close to 100 specimens/kg of sample. Ostracods and crinoids are rare, 1–2 specimens/kg of sample. In contrast, the dacryoconarid proportion in every sample is of several hundred per kilogram. Only the pectiniform conodont elements (P elements) were studied in detail in this work.

4.2 Conodonts

Sample PE-A/4 was the only productive sample from the PE-A section, yielding a single identifiable P element attributed to *Polygnathus* aff. *partitus* (Fig. 4a). Most samples from the PE-B section were productive, leading to the identification of nine species, from two genera (*Polygnathus* and *Tortodus*) (Table 1). *P. costatus* appears throughout the section, with the exception of the uppermost sample (PE-B/13). *P. angustipennatus* is also widely distributed, from samples PE-B/4 to PE-B/10. All other species occur occasionally (Table 1). In section PE-B, *Polygnathus* species diversity (eight species) dominates over *Tortodus* (one species), and below sample PE-B/12, the assemblage is constituted solely by *Polygnathus* species. Assemblages from the PE-B section are poorly diversified throughout the section, reaching a maximum of three species in samples PE-B/4 and PE-B/12.

Section PE-C has the highest diversity in respect to both species (11) and genera (3) (Table 2). Five of the species occurring in section PE-B are also present in this section: *Polygnathus costatus*, *P. angusticostatus*, *P. angustipennatus*, *P. oblongus* and *Tortodus australis* (Table 2). Three other species of *Polygnathus* are present in this section, one with a broad distribution, *P. pseudofoliatius* (samples PE-C/5 to PE-C/9), and *P. trigonicus* and *P. ensensis* in sample PE-C/9 (Table 2). A second species of *Tortodus*, *T. kockelianus*, has its first occurrence in sample PE-C/8 and occurs continuously until the uppermost sample (PE-C/12). Two species of *Icriodus* (*I. rectirostratus* and *I. regularicrescens*) were identified, both in sample PE-C/6. The diversity throughout the section is mostly low (0–3 species), being higher in samples PE-C/6 (three genera, seven species), PE-C/9 (two genera, four species) and PE-C/9 (two genera, seven species).

5 Conodont systematic paleontology

Class Conodonta Pander, 1856

Icriodus Branson & Mehl, 1933

Icriodus rectirostratus Bultynck, 1970

Figure 4ao–ap.

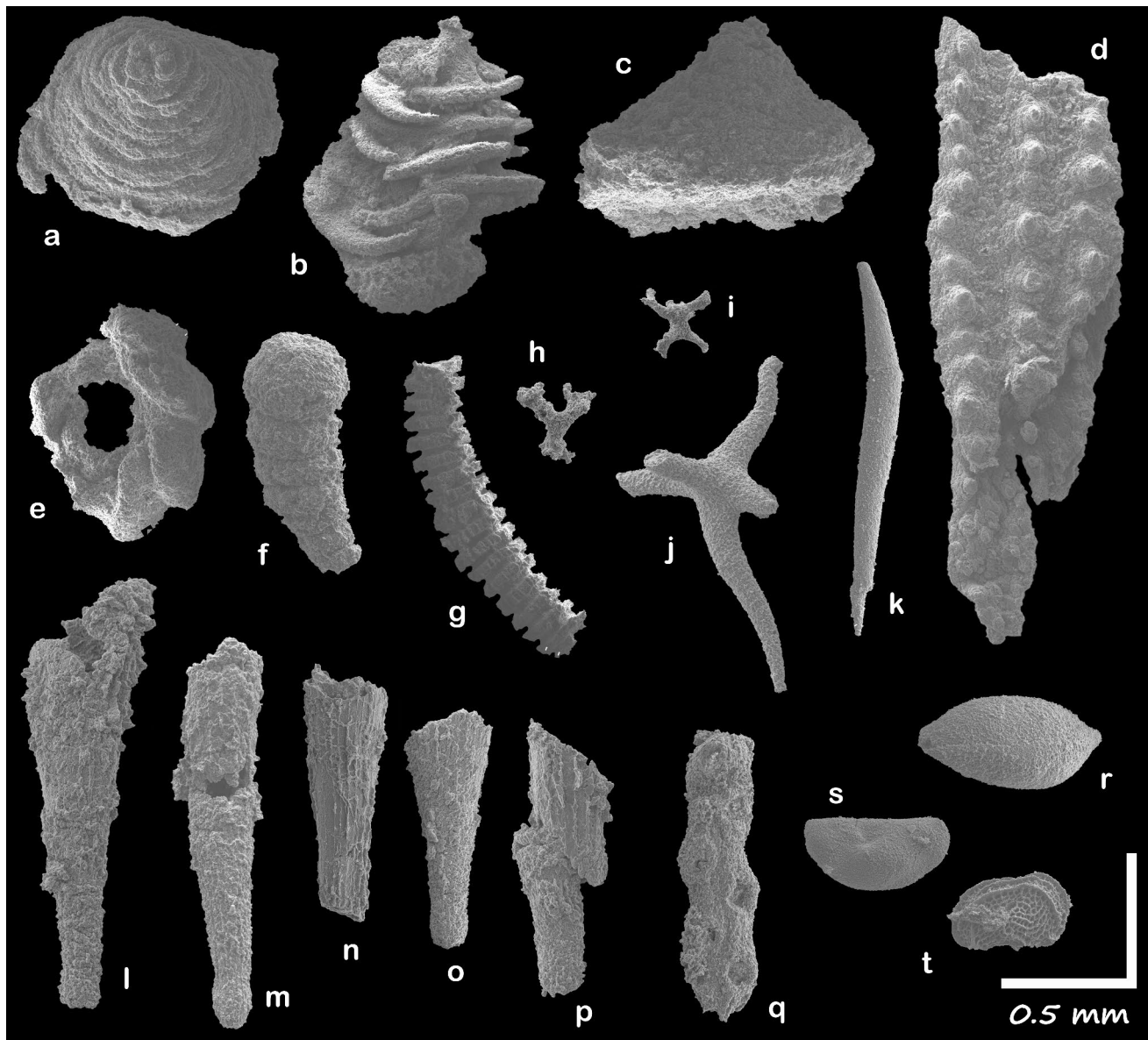


Fig. 3 Examples of microfossils, other than conodonts, found in the Pedreira da Engenharia section. **a–c**: fossils of uncertain group; **a–b** from sample PE-A/2; **c** from sample PE-A/5. **d**: crustacean plate (?), from sample PE-A/2. **e–f**: foraminifers, from sample PE-A/5. **g–k**: sponge spicules; **g** from sample PE-A/2; **h, i** from sample PE-B/9;

j, k from sample PE-C/6. **l–p**: dacryoconarids; **l** and **p** from sample PE-B/5; **m** from sample PE-C/6; **n** from sample PE-B/7; **o** from sample PE-B/1. **q**: bryozoan, from sample PE-B/11. **r–t**: ostracods; **r** from sample PE-C/6; **s, t** from sample PE-C/2

1970 *Icriodus nodosus rectirostratus* n. subsp. – Bultynck, pl. III, Fig. 1, pl. XXX, figs. 7–8.

1977 *Icriodus corniger rectirostratus* – Weddige, pl. 1, figs. 7–9.

Material – 1 specimen, from sample PE-C/6.

Description – Element with a wide, hook shape (in upper view), even height throughout and horizontally straight. The spurn is smooth, its anterior margin meets the platform at a right angle, and it is much smaller than the outer expansion of the basal cavity, which is wider than the main body and

convex. The posterior extension of the middle row is straight and slightly deflected outwards. The lateral rows are straight, parallel and symmetrical relative to the middle row in the four posterior denticles, with the ones from the middle row being taller than those of the lateral rows. In this section of the four posterior denticles, the denticles of the lateral rows are almost aligned with the ones on the middle row. The lateral denticles in the transverse rows are separated by deep grooves and connected with the middle row by thin and short transverse ribs. The following two denticles of each lateral

row are much larger than the previous ones, taller and wider than the ones on the middle row, and deflected inwards. The inner row ends with these denticles, while the middle and outer rows continue anteriorly and fuse together, following the same deflected pattern from the previous set.

Discussion – Although the lower side of the single found specimen was not photographed under the SEM microscope, the right angle of the inner process, the straight posterior extension of the middle row, the deflected blade and the increased dimension of the first two denticles in the anterior end of the lateral rows lead us to attribute this specimen to *I. rectirostratus*.

Biostratigraphic range – *partitus* to *costatus* zones.

Icriodus regularicrescens Bultynck, 1970

Figure 4ab

1970 *Icriodus regularicrescens* n. sp. – Bultynck, pl. VII, figs. 1–7, pl. VIII, figs. 2, 4, 7–8.

1987 *Icriodus regularicrescens* Bultynck, 1970 – Bultynck, pl. 4, figs. 1–3, 11.

Material – 1 specimen, from sample PE-C/6.

Description – Narrow, elongated element, with a somewhat lenticular shape. The anterior third of the middle row is composed of isolated high denticles, directed upwards. There is a tiny spurn and a larger and convex expansion on the outer side. The transverse rows are straight and parallel, with denticles slightly increasing in size anteriorly. The lateral rows are symmetrical relative to the middle row. Lateral denticles are almost aligned with the middle ones, separated from successive rows by deep grooves and connected with the middle row by thin and short transverse ridges. Posterior extension of the middle row consists of three straightly disposed denticles.

Discussion – The symmetrical disposition of the rows, the narrow body and the straight posterior extension of the middle row in this specimen resemble the ones illustrated by Bultynck (1970), however, ours presents a prominent, upwardly directed, free blade.

Biostratigraphic range – *costatus* (Belka et al., 1997) to *varcus* (Liao & Valenzuela-Ríos, 2008) zones.

Polygnathus Hinde, 1879

Polygnathus angusticostatus Wittekindt, 1965.

Figure 4t–w and ad–af.

1965 *Polygnathus angusticostata* n. sp. – Wittekindt, pl. 1, figs. 15–18.

1971 *Polygnathus angusticostatus* Wittekindt, 1966 – Klapper, pl. 3, figs. 21–25.

1972 *Polygnathus angusticostatus* Wittekindt, 1965 – Boogaard, pl. 1, fig. b.

2011 *Polygnathus angusticostatus* Wittekindt, 1966 – Walliser & Bultynck, pl. 2, figs. 3–4.

2013 *Polygnathus angusticostatus* Wittekindt, 1966 – Liao & Valenzuela-Ríos, Fig. 7B.

Material – 8 specimens, from samples PE-B/6 (1), PE-C/5 (3), PE-C/6 (1), PE-C/8 (1) and PE-C/9 (2).

Description – Free blade long, close to 1/2 of the total length. The platform is rectangular to drop-shaped. The posterior end of the carina is usually free, possessing 2 to 3 denticles. In some cases, the platform margins develop acutely into the posterior tip (specimens ad and ae). Platform is generally wide, symmetrical, with the posterior third slightly twisted interiorly and the anterior outer margin being elevated, generating a recurved shape of the outer margin. Shallow adcarinal grooves are present anteriorly and gradually disappear posteriorly. The margins are ornamented with nodes, which can combine to form short ridges, ending midway to the carina.

Discussion – The free posterior end are shared characteristics of *P. angusticostatus* and *P. angustipennatus*. The wide, unconstricted and curved shape of the platform distinguish *P. angusticostatus* from *P. angustipennatus*. Specimens v and ad do not have symmetrical platforms, however, they have a free posterior end and a wide unconstricted platform, similar to the remaining figured specimens. Specimen af has an atypically long free blade for the species, but its wide unconstricted platform and the free posterior end are characteristic of *P. angusticostatus*.

Biostratigraphic range – *costatus* to *hemiansatus* zones (Walliser & Bultynck, 2011).

Polygnathus angustipennatus Bischoff & Ziegler, 1957

Figure 4n–s

1957 *Polygnathus angustipennata* n. sp. – Bischoff & Ziegler, pl. 3, figs. 1–3.

1971 *Polygnathus angustipennatus* Bischoff & Ziegler, 1957 – Klapper, pl. 3, Fig. 27.

1987 *Polygnathus angustipennatus* Bischoff & Ziegler, 1957 – Bultynck, pl. 9, Fig. 15.

2011 *Polygnathus angustipennatus* Bischoff & Ziegler, 1957 – Walliser & Bultynck, pl. 2, figs. 5a–5b.

2013 *Polygnathus angustipennatus* Bischoff & Ziegler, 1957 – Liao & Valenzuela-Ríos, Fig. 7A.

Material – 14 specimens, from samples PE-B/4 (1), PE-B/10 (1), PE-C/5 (2), PE-C/6 (6), PE-C/8 (1), PE-C/9 (2) and PE-C/12 (1).

Description – Free blade long and tall (best seen in specimens n, q and s), generally over 1/2 of the total length. The shape of the platform is rectangular to triangular. The posterior end of the carina is free, possessing 2 to 3 denticles. Platform is generally constricted, symmetrical, with straight and parallel margins in the anterior half, and with the posterior third slightly twisted interiorly, ending acutely with the carina. Shallow adcarinal grooves are present throughout the platform. The margins are ornamented with small nodes, which can combine to form short ridges, restricted to the margins.

Discussion – The slender, constricted shape of the platform and the long and tall free blade distinguish it from *P. angusticostatus*.

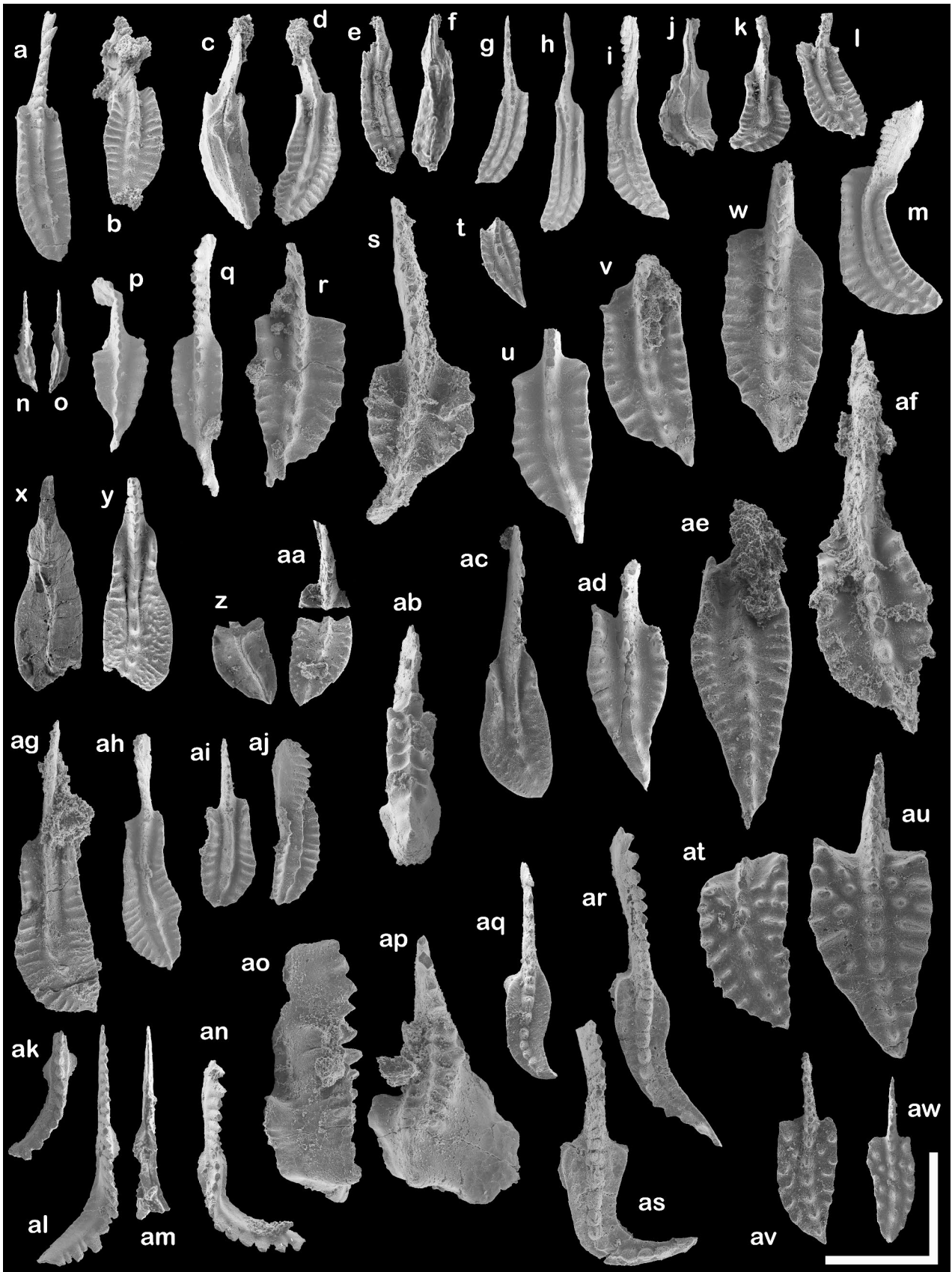


Fig. 4 Pectiniform elements from the PE section. *P.* = *Polygnathus*; *T.* = *Tortodus*; *I.* = *Icriodus*. **a–b**: *P. partitus*; **a** *P. aff. partitus*, from sample PE-A/4; **b** from sample PE-B/4; **c–i**: *P. costatus*; **c, d** lower and upper view, respectively, of specimen from sample PE-B/1; **e, f** upper and lower view, respectively, of specimen from sample PE-B/12; **g–i** from sample PE-C/6. **j, k**: *P. cf. karapetovi*, lower and upper view, respectively, of specimen from sample PE-B/10. **l, m**: *P. oblongus*; **l** from sample PE-B/4; **m** from sample PE-C/6. **n–s** *P. angustipennatus*; **n, o** upper and lower view, respectively, of specimen from sample PE-B/10; **p** from sample PE-C/9; **q** from sample PE-C/6; **r** from sample PE-C/5; **s** from sample PE-C/8. **t–w** and **ad–af**: *P. angusticostatus*; **t** from sample PE-B/6; **u** from sample PE-C/6; **v, w** from sample PE-C/5; **ad–ae** from sample PE-C/9; **af** from sample PE-C/8. **x–y**: *P. cf. pseudoeiflius*, lower and upper view, respectively, of specimen from sample PE-B/13. **z–aa**: *P. benderi*, lower and upper view, respectively, of specimen from sample PE-B/12. **ab**: *I. regularicrescens*, from sample PE-C/6. **ac**: *P. ensensis*, from sample PE-C/9. **ag–aj**: *P. pseudofoliatus*: **ag** from sample PE-C/8; **ah** from sample PE-C/9; **ai, aj** upper and lateral view, respectively, of specimen from sample PE-C/5. **ak–an**: *T. australis*; **ak** from sample PE-C/9; **al, am** upper and lower view, respectively, of specimen from sample PE-B/12; **an** from sample PE-C/6. **ao, ap**: *I. rectirostratus*, lateral and upper view, respectively, of specimen from sample PE-C/6. **aq–as**: *T. kockelianus*; **aq** from sample PE-C/9; **ar, as** from sample PE-C/8. **at–aw**: *P. trigonicus*, from sample PE-C/9. Scale bar = 0.5 mm

Biostratigraphic range – *costatus* (Belka et al., 1997) to *hemiansatus* (Bultynck, 1987) zones.

Polygnathus benderi Weddige, 1977

Figure 4z–aa.

1977 *Polygnathus benderi* n. sp. – Weddige, pl. 3, Fig. 59–61.

2011 *Polygnathus benderi* Weddige, 1977 – Vodrážková et al., Fig. 11E, F, H, J–L.

Material – 1 specimen, from sample PE-B/12.

Description – Free blade short (however, the tip is fractured in the figured specimen, so it can be longer), tall, and slightly curved inwards. Its denticles are conical, free on the tips and of elliptic section. The main body has a falcate shape, almost symmetrical, slightly curving inwards and then outwards in the posterior end. The inner margin is straight in the anterior 2/3 of the body and convex in the last 1/3. The outer margin is smoothly convex throughout all its length. In the anterior end the inner margin meets the carina at a right angle and in a slightly more anterior position than the outer margin, while the latter meets the carina smoothly. The denticles of the anterior half of the main body are low, conical and partially fused, while the ones of the posterior half are much smaller and rounded, maintaining their size towards the posterior end, meeting the tip. The upper side of the platform is poorly ornamented. The outer half of the platform has small nodes throughout its length, while the inner one has the same kind of nodes on the posterior half, but fine ridges on the anterior one. The ridges are perpendicular to the carina and separated from it by a very smooth adcarinal groove, which is present only in association with

the ridges. The basal pit was damaged during preparation, but it is possible to say that it is located in the anterior end of the main body. It continues, posteriorly, as a low and sulcate thick keel that extends until the posterior tip.

Discussion – The poor ornamentation, composed almost entirely by nodules, the lack of well-marked adcarinal grooves and the smooth curvature of the outer and inner margins distinguish it from the similar *P. eiflius*.

Biostratigraphic range – *costatus* to *australis* zone (Bardashev, 1992).

Polygnathus costatus Klapper, 1971

Figure 4b–i

1971 *Polygnathus costatus costatus* subsp. nov. – Klapper, pl. 1, Fig. 30–36; pl. 2, fig. 1–7.

2009 *Polygnathus costatus costatus* Klapper, 1971 – Berkyová, Fig. 6 I–L.

Material – 19 specimens, from samples PE-B/1 (1), PE-B/2 (1), PE-B/5 (1), PE-B/12 (1), PE-C/2 (4), PE-C/6 (11).

Description – Free blade short, tall, straight, oriented slightly inwards and representing about 1/3 of the whole length. Its denticles are conical, free on the tips, of elliptic section and identical size. The main body is constricted in the anterior end, expanding at the anterior third and then shortening again into a tip on the posterior end. It is almost symmetrical in respect to the carina and curves slightly inwards. Both inner and outer margins are straight and parallel in the anterior 1/3 and convex in the rest of the body, with the outer margin being slightly more expanded at mid-length. In the anterior end, the margins bend upwards in an angle that slightly exceeds 90° and meet the carina in a right angle. The denticles of the anterior half of the main body are short, rounded and almost completely fused together, while the ones in the posterior half are also short and rounded, but are isolated and their size diminishes towards the posterior end, reaching the tip. The upper side of the platform has thin transversal ridges that reach the carina, being separated from it by very well-marked adcarinal grooves, which are very deep in the anterior end and shallow in the posterior one. The ridges are separated by smooth grooves and oriented perpendicularly to the carina in the anterior half of the main body, while being radial in the posterior half. In lateral view, the element has a shape similar to that of an axe-head, with the free blade being of triangular shape and the main body short and bent in the posterior end (≈ 40°). The basal pit is small, almost circular, symmetrical and located at the anterior 1/4 of the main body. It continues, anteriorly and posteriorly, as keels, with the posterior one being always of the same height, while the anterior one increases its height towards the anterior end.

Discussion – The slender shape of the platform, convex margins and the constricted anterior margin of the main

body distinguish *P. costatus* from the similar *P. patulus* and *P. partitus*.

Biostratigraphic range – *costatus* (Bardashev, 1992) to *australis* (Berkyová, 2009) zones.

Polygnathus ensensis Ziegler & Klapper, in Ziegler et al., 1976

Figure 4ac

1976 *Polygnathus xylus ensensis* n. subsp. – Ziegler & Klapper, pl. 3, figs. 4–9.

1987 *Polygnathus ensensis* Ziegler & Klapper, 1976 – Bultynck, pl. 7, figs. 1–6.

2011 *Polygnathus ensensis* Ziegler & Klapper, 1976 – Walliser & Bultynck, pl. 1, figs. 21–22.

Material – 1 specimen, from sample PE-C/9.

Description – Free blade long, about 1/2 of the total length, straight and high. The platform is constricted in the anterior third, developing strong troughs with four denticles on each margin. The margins on the anterior end are parallel. In both margins, the first three denticles are more developed than the fourth and are aligned. The fourth denticle is flexed outwards relative to the alignment of the remaining denticles. Deep adcarinal grooves are present in the anterior third of the platform, disappearing at midlength. The platform greatly expands at midlength, with the outer margin being more expanded, ornamented by small nodes on the surface, close to the margins, and curved downwards posteriorly. The carina is composed of thick, fused denticles in the anterior half, while the posterior half has isolated, small and widely spaced nodes that reach the posterior end.

Discussion – Although similar to *P. eiflius* and *P. timorensis*, this specimen can be attributed to *P. ensensis* due to its characteristic troughs on both sides of the constricted anterior third of the platform, with straight margins, discrete denticles on each margin, and the downwards curve of the platform posteriorly.

Biostratigraphic range – *ensensis* (Walliser & Bultynck, 2011) to *ansatus* (Bultynck, 1987) zones.

Polygnathus cf. *karapetovi* Bardashev, 1991

Figure 4j-k

1985 *Polygnathus costatus* subsp. nov. b (*P. c. karapetovi*) – Bardashev & Ziegler, pl. 1, figs. 8–9.

1992 *Polygnathus costatus karapetovi* – Bardashev, pl. 1, Fig. 32.

Material – 1 specimen, from sample PE-B/10.

Description – The free blade of the specimen is incomplete, but is tall, straight, slightly oriented externally and representing at least 2/5 of the whole length. Its denticles are conical, free on the tips, of elliptic cross section and identical size. The main body is slightly constricted in the anterior end and expands abruptly at the remainder of its length, reducing its width only at the posterior tip. It is symmetrical in respect to the carina, curves abruptly to the inner side ($\approx 80^\circ$) at 3/5 from the posterior end of the main body and then

recurves at 1/5 from the same end, in a 20° angle. The anterior ends of both inner and outer margins are straight and parallel to the carina, however, the inner margin ends more anteriorly than the outer one. The posterior 6/7 of the outer margin is strongly convex (almost circular), recurving only at the posterior tip. The inner margin is straight in the anterior 1/7, makes a small but abrupt curve towards the carina, then becomes straight until the anterior 4/7 of the body, oriented away from the carina at an angle of around 20° . The posterior 3/7 of the inner margin is strongly convex. In the anterior end the margins bend upwards in an angle that does not exceed 50° and meet the carina smoothly. The denticles of the anterior half of the main body are short, conical and completely fused, while the ones in the posterior half are short, rounded, isolated and of the same size until reaching the posterior tip. The upper side of the platform has thin transversal ridges that almost reach the carina, being separated from it by very well-marked adcarinal grooves, which are deep in the anterior end and shallow in the posterior one. The ridges are separated by smooth grooves and are oriented radially. The basal cavity is relatively large, elliptical, symmetrical and located at the anterior end of the main body. It continues, anteriorly and posteriorly, as well-marked keels that reach both ends.

Discussion – The high angle of curvature of the platform, the even size of the denticles in the carina, the connection of the inner and outer margins with the carina at different distances from the anterior end, the locally strong convexity of the margins, the smaller angle of the anterior bent of the platform and the more anterior location of the basal pit distinguish this specimen from *P. costatus* and *P. partitus*.

Biostratigraphic range – *costatus* to *australis* zones (Bardashev, 1992).

Polygnathus partitus Klapper et al., 1978

Figure 4a-b

1978 *Polygnathus costatus partitus* subsp. nov. – Klapper et al., pl. 2, figs. 1–5, 13.

2009 *Polygnathus costatus partitus* Klapper et al., 1978 – Berkyová, fig. 5D-I.

Material – 2 specimens, from samples PE-A/4, and PE-B/4.

Description – Free blade tall, straight and representing about 2/5 of the whole length. Its denticles are conical, free on the tips and of elliptic cross section. The main body is slightly constricted on the anterior end, expanding at mid length of the platform and ending sharply in the posterior end. It is almost symmetrical in respect to the carina and curves slightly inwards. Both margins are straight and parallel in the anterior 1/3 and the outer margin is convex in the rest of the body, with the expansion being the largest at mid length of the main body (slightly more posteriorly in specimen a). The denticles of the anterior half of the main body are tall, conical and completely fused, while the ones

in the posterior half are rounded and isolated, with their size diminishing towards the posterior end, reaching the tip (specimen a, visible; specimen b, unclear). The upper side of the platform has thin transversal ridges that reach the carina, being separated from it by well-developed adcarinal grooves, which are very deep in the anterior end and diminish at about 1/4 to the posterior one.

Discussion – The slightly less constricted anterior margins of the platform, the absence of adcarinal grooves in the posterior end and the less developed ridges differentiate it from *P. costatus*. The extension of the carina to the posterior end distinguishes it from *P. patulus*. Because specimen a is largest past mid-length of the platform posteriorly it is considered as *P. aff. partitus*.

Biostratigraphic range – *partitus* (Bardashev, 1992) to *costatus* (Berkyová, 2009) zones.

Polygnathus oblongus Weddige, 1977

Figure 4l-m

1977 *Polygnathus costatus oblongus* n. ssp. – Weddige, pl. 4, Fig. 71, 72.

2013 *Polygnathus oblongus* Weddige, 1977 – Liao & Valenzuela-Ríos, Fig. 7F, G.

Material – 3 specimens, from samples PE-B/4 (1) and PE-C/6 (2).

Description – The free blade is short, less than 1/3 of the length, straight and slightly tilted inwards. The main body is slightly constricted in the anterior end (more internally than externally), having a smooth expansion until the posterior third, where it starts narrowing into a tip. It is almost symmetrical and strongly curved inwards. Both inner and outer margins are straight in the anterior 1/3 and convex in the rest of the body, with the outer margin being slightly more expanded at the posterior 1/3 of the length. The denticles in the anterior half of the carina are slender and fused, while the ones in the posterior half are rounded and isolated, with their size diminishing towards the posterior end, reaching the tip. The upper side of the platform has thin transversal ridges that almost reach the carina, being separated from it by very well-developed adcarinal grooves, which are deep in the anterior end and shallow in the posterior one. The ridges are separated by smooth grooves and oriented perpendicularly to the carina throughout the main body.

Discussion – The outwards projection of the anterior end of the outer margin of the platform distinguishes this specimen from any other taxon of the *P. costatus* group. The smooth curvature of both the inner and outer margins is similar to that of *P. costatus* and *P. patulus*, but the platform has a lesser expansion in those species.

Biostratigraphic range – *costatus* (Bardashev, 1992) to *kockelianus* (Weddige, 1977) zones.

Polygnathus cf. pseudoeiflius Walliser & Bultynck, 2011

Figure 4x-y

2011 *Polygnathus pseudoeiflius* n. sp. – Walliser & Bultynck, pl. 1, figs. 3–5.

Material – 1 specimen, from sample PE-B/13.

Description – The free blade is fractured but some conical denticles, free on the tips and of elliptic cross section, are visible. The main body is constricted in the anterior end, expanding at the anterior 1/3 and then shortening again posteriorly. Posterior end is broken. It is asymmetrical, with the outer platform being more expanded, and bends inwards ($\approx 40^\circ$) in the posterior 1/4. Both the inner and outer margins are straight and parallel on the anterior 1/3, forming a rostrum, and convex in the rest of the body, with the inner margin presenting a very small curvature, while the outer margin curves outwards at mid length and inwards in the posterior end. In the anterior end the margins bend upwards in an angle that does not exceed 90° and meet the free blade smoothly. The denticles of the anterior half of the carina are short, conical and almost completely fused, while the ones in the posterior half are also short, but rounded and isolated, with their size diminishing towards the posterior end. The upper side of the platform has thin and short ridges and small rounded nodules, disposed randomly and abundantly throughout the platform. It exhibits very thin and deep adcarinal grooves, which are deeper in the anterior end and virtually absent in the posterior 1/3. The basal pit is small, elliptical, symmetrical and located at the anterior 1/4 of the main body. It continues, posteriorly, as a low keel, possibly reaching the posterior end (not preserved).

Discussion – The ornamentation composed by nodules and the high proportion in which they appear distinguish it from the *P. costatus* group. A straight rostrum at the anterior third, instead of a diagonal one, distinguishes *P. pseudoeiflius* from *P. eiflius*. Although this specimen has a straight rostrum, its platform is more slender than the type specimens figured in Walliser and Bultynck (2011).

Biostratigraphic range – *kockelianus* to *timorensis* zones (Walliser & Bultynck, 2011).

Polygnathus pseudofoliatus Wittekindt, 1965.

Figure 4ag-aj.

1965 *Polygnathus pseudofoliata* n. sp. – Wittekindt, pl. 2, figs. 19–23.

1971 *Polygnathus pseudofoliatus* Wittekindt, 1966 – Klapper, pl. 2, figs. 8–13.

1987 *Polygnathus pseudofoliatus* Wittekindt, 1965 – Bultynck, pl. 8, figs. 19–20.

2009 *Polygnathus pseudofoliatus* Wittekindt, 1966 – Berkyová, Fig. 8 A-G.

2011 *Polygnathus pseudofoliatus* Wittekindt, 1966 – Walliser & Bultynck, pl. 1, figs. 1–2.

Material – 3 specimens, from samples PE-C/5 (1), PE-C/8 (1) and PE-C/9 (1).

Description – Free blade short, around a third of the total length. The platform is asymmetrical, with straight and

parallel margins in the anterior third, expanding posteriorly with a maximum at the posterior third. The inner margin is convex and one specimen (ah) presents a protrusion at its mid length. The outer margin is straight in the anterior part and then convex posteriorly. The margins are mostly elevated at 1/3 of the anterior end of the platform, widening both anteriorly and posteriorly. The anterior end of the margins dips down and opens on the outer side. There are deep adcarinal grooves in the anterior third of the platform, becoming shallower and narrower towards the posterior tip. The carina is composed of fused denticles throughout the platform, decreasing in height posteriorly and ending at the posterior end. Strong and unevenly spaced transverse ribs are present in both margins of the platform, almost reaching the carina.

Discussion – The unevenly spaced transverse ribs, the relatively unstricted anterior end and the strong asymmetry of the platform distinguish these specimens from *P. costatus*.

Biostratigraphic range – *costatus* (Belka et al., 1997) to *rhenanus* (Bultynck, 1987) zones.

Polygnathus trigonicus Bischoff & Ziegler, 1957

Figure 4at-aw.

1957 *Polygnathus trigonica* n. sp. – Bischoff & Ziegler, pl. 5, figs. 1–6.

1965 *Polygnathus trigonica* Bischoff & Ziegler, 1957 – Wittekindt, pl. 3, Fig. 1.

1985 *Polygnathus trigonicus* Bischoff & Ziegler, 1957 – Bardashev & Ziegler, pl. 1, Fig. 20.

2009 *Polygnathus trigonicus* Bischoff & Ziegler, 1957 – Berkyová, Fig. 6D.

2011 *Polygnathus trigonicus* Bischoff & Ziegler, 1957 – Walliser & Bultynck, pl. 2, Fig. 6.

Material – 4 specimens, from sample PE-C/9.

Description – Free blade short, less than a third of the total length. The platform is mostly symmetrical, triangularly shaped, widest at the anterior end and gradually shrinks until reaching the posterior end in a tip. It bends down anteriorly, meeting the carina at a right angle. The carina is composed of rounded and isolated denticles that reach the posterior end. The surface of the platform is ornamented by large nodes, disposed symmetrically relative to the carina and fused together to form ridges in larger specimens. A symmetrical set of nodes in the anterior end of the platform make a triangular shape, opened anteriorly, which marks the end of the ornamentation of the platform anteriorly. The surface between the nodes and ridges is flat. The platform is curved downwards, posteriorly. The basal pit is small, elliptic, symmetric, located almost at the anterior end of the platform and develops into a keel that extends to the posterior end.

Discussion – The well-developed platform, reaching the posterior end distinguishes these specimens from *P.*

angusticostatus. The large diagonal nodes and ridges, the triangular shape of both the platform and the area without ornamentation and the location of the basal pit close to the anterior margin distinguish these specimens from other *Polygnathus* species.

Biostratigraphic range – *australis* (Belka et al., 1997) to *ensensis* (Walliser & Bultynck, 2011) zones.

Tortodus Weddige, 1977

Tortodus australis (Jackson in Pedder et al., 1970).

Figure 4ak-an.

1970 *Polygnathus kockelianus australis* subsp. nov. – Jackson, in Pedder et al., 1970, pl. B, Fig. 22, 25.

1985 *Tortodus kockelianus australis* Jackson, 1970 – Bardashev & Ziegler, pl. 2, Fig. 23.

2009 *Tortodus kockelianus australis* (Jackson, 1970) – Berkyová, Fig. 6 H.

2010 *Tortodus kockelianus australis* (Jackson, 1970) – Machado et al., pl. 2, figs. N-P.

Material – 3 specimens, from samples PE-B/12 (1), PE-C/6 (1) and PE-C/9 (1).

Description – Free blade long, high, straight and representing about 1/2 of the whole length. Its denticles are conical, completely free, of elliptic cross section and of identical size. The main body is very thin, elongated, ending in a tip and curved inwards and twisted down at an angle ranging from 35° to 70°. Both inner and outer margins are parallel to the carina throughout the whole length. The denticles are similar to those of the free blade, although their size changes in a seemingly random way throughout the carina, until reaching the posterior end. The platform is restricted to a short expansion of the element at the base of the carina, with no ornamentation. The basal cavity is large, elliptical, asymmetrical, with the outer side being more developed, and located at the anterior end of the main body. It continues as a narrow and deep groove, on both sides, reaching the posterior end, but turning into a keel in the anterior one.

Discussion – The high denticles throughout the carina, the bent posterior end and the large basal cavity assign it to genus *Tortodus*, rather than to *Polygnathus*. The poorly developed platform distinguishes it from other *Tortodus* species.

Biostratigraphic range – *australis* to *kockelianus* zones (Bardashev & Ziegler, 1985).

Tortodus kockelianus (Bischoff & Ziegler, 1957).

Figure 4aq-as.

1957 *Polygnathus kockeliana* n. sp. – Bischoff & Ziegler, pl. 2, figs. 1–8.

1985 *Tortodus kockelianus kockelianus* (Bischoff & Ziegler, 1957) – Bardashev & Ziegler, pl. 2, Fig. 22.

1987 *Tortodus kockelianus kockelianus* (Bischoff & Ziegler, 1957) – Bultynck, pl. 9, Fig. 17.

2009 *Tortodus kockelianus kockelianus* (Bischoff & Ziegler, 1957) – Berkyová, Fig. 6 A-C, E-G.

Material – 11 specimens, from samples PE-C/8 (2), PE-C/9 (3), PE-C/10 (1), PE-C/11 (1) and PE-C/12 (4).

Description – Free blade long, representing about 1/2 of the whole length, tall and with conical denticles of elliptic cross section. The main body is wide, anteriorly, elongated and reaching the posterior end, which is curved inwards and twisted down in an angle ranging from 40° to over 90°. Both inner and outer margins are parallel to the carina throughout the whole length. The denticles of the carina are conical and of circular section in the anterior half, gradually becoming elliptic posteriorly. The platform is wide, with no ornamentation and margins slightly elevated.

Discussion – The well-developed, symmetrical, platform, with no ornamentation, that reaches the posterior end distinguishes it from other *Tortodus* species.

Biostratigraphic range – *kockelianus* to *ensensis* zones (Bardashev & Ziegler, 1985).

6 Discussion

6.1 Conodont biostratigraphy

The new data obtained in this study adds to the work of Boogaard (1972), who processed samples collected only at the quarry floor. However, the results we obtained from the current quarry floor (PE-A section), now inactive, strongly contrast with the ones obtained by Boogaard. In his work, Boogaard identified three species of *Polygnathus* (*P. angusticostatus*, *P. costatus* and *P. linguiformis*) and two undetermined species of *Icriodus*, which place this section in the *costatus* zone. In our study, only a single specimen of *P. aff. partitus* was identified in the PE-A section. Although *P. partitus* is the index species of the *partitus* zone (first zone of the Eifelian), its range extends into the *costatus* zone, thus, a single identifiable specimen could belong to either zone. It is possible that the current quarry floor is at a lower level than the one at the time of Boogaard's work, and, since the layers generally dip 50 °NE (Theias et al., 2018), the sampled layers may be stratigraphically below the ones processed by Boogaard. We consider that the PE-A section either belongs to the *partitus* or to the *costatus* zones, in the lower part of the Eifelian (Fig. 5).

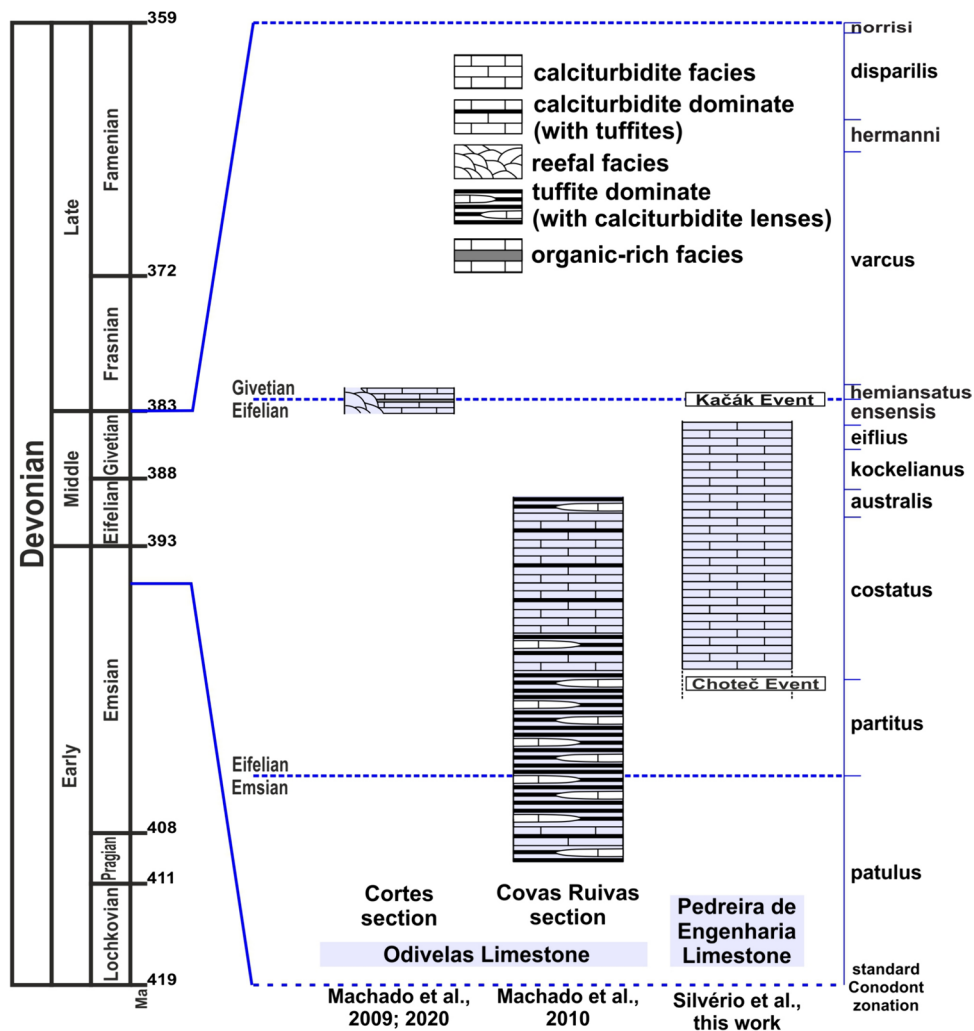
The results from the PE-B section are much more in line with what Boogaard found in his work. There is a clear predominance of *P. costatus*, the index species of the *costatus* zone, from the lowermost sample (PE-B/1) upwards. This limits the base of the sequence to the *costatus* zone. The index species for the following zone is *Tortodus australis*, found in sample PE-B/12, which places the boundary between the two zones at the base of the corresponding bed. The boundary may be stratigraphically lower, since no identifiable element was found in sample PE-B/11. In this case,

P. partitus, in sample PE-B/4, marks the boundary between the two zones, since this species is only found in the *costatus* zone. A similar situation is evidenced by the presence of *P. cf. pseudoeiflius* (Fig. 4x, y) in sample PE-B/13, which, if its identification is confirmed, marks the boundary between the *australis* and *kockelianus* zones, since the first appearance datum of *P. pseudoeiflius* is within the *kockelianus* zone. That would mean that the *australis* zone is represented in the PE-B section by a maximum of one meter (thickness between samples PE-B/11 and PE-B/13). However, such assumption would be poorly based, since there is only one identifiable specimen in sample PE-B/13 and does not correspond to the index species of the *kockelianus* zone. Given the overall results, we find it best to place the boundary between the *costatus* and *australis* zones at the base of the level of sample PE-B/12 and consider these to be the only two biozones present in the sequence, as illustrated in Fig. 2d.

In section PE-C, almost the entire Eifelian seems to be represented, apart from the *partitus* zone (first zone of the Eifelian). The assemblages are in accordance with the *costatus* zone from samples PE-C/2 to PE-C/5. Because this zone spans over 13 m in section PE-B, it is safe to assume that sample PE-C/1 can be assigned to the *costatus* zone, despite its lack of identifiable elements. This gives an approximate 5 m thickness to the *costatus* zone in section PE-C. Similar to section PE-B, the boundary between the *costatus* and *australis* zones is marked by the appearance of *Tortodus australis*, in sample PE-C/6. The presence of one specimen of *I. rectirostratus* (a species which does not reach the *australis* zone) in sample PE-C/6 may be due to this being a reworked specimen, or because the sample contained the boundary between the two zones, resulting in the mixing of species from both zones. The appearance of *T. kockelianus* in sample PE-C/8 marks the base of the *kockelianus* zone. Less than a meter higher, the appearance of *P. ensensis* in sample PE-C/9 marks the beginning of the *ensensis* zone. Since the upper part of the Eifelian is subdivided into four successive zones (*australis*, *kockelianus*, *eiflius* and *ensensis*), the *eiflius* zone should also be present in the section, between the beds of samples PE-C/8 and PE-C/9, assuming the absence of a hiatus. The maximum thickness for both the *kockelianus* and *eiflius* zones in section PE-C is approximately 1.5 m (distance between samples PE-C/7 and PE-C/9; Fig. 2d). Either the *eiflius* zone is not present in the section, or it is condensed in this part of the sequence. No novel species appear after sample PE-C/9, although both *P. angustipennatus* and *T. kockelianus* range beyond the *ensensis-hemiansatus* boundary (Eifelian-Givetian boundary). In the present work, we limit the PE-C section to the *ensensis* zone, not reaching *hemiansatus*.

We could not determine biozones for the PE-A section, since most of the section is covered by sediment and

Fig. 5 Schematic stratigraphic profiles of SW Ossa Morena Zone Devonian limestones sections (adapted from Moreira et al., 2021). Numerical ages are as indicated by Cohen et al. (2023). Age of Choteč Event in accordance with Becker and Aboussalam (2013), Koptíková (2011) and Vodrážková et al. (2012)



vegetation, but assume stratigraphic and structural continuity between this and the remaining sections. For the PE-B section, much of its thickness is attributed to the *costatus* zone (> 13 m), coinciding with the folded part of the section (see S_0 pattern illustrated in Fig. 2a). The deformation was taken into account during the elaboration of the stratigraphic column for this section, however, some layers may be duplicated, given the difficulty in assessing the precise orientation of each stratum in the quarry face from a distance. Section PE-C shows no sign of deformation in the field, and there is no evidence of biozone duplication or tectonic overthickening of the succession.

The changes in conodont species diversity of section PE-C appear to be linked to the biozone boundaries. The results show the diversity increasing each time there is a biozone change. This is especially evident in the *costatus* to *australis* and *kockelianus* to *ensensis* transitions. These increases in diversity may be linked to speciation events, although, it is also plausible that these are artifacts from the sampling. A large number of specimens, preferably hundreds

per sample, would confer statistical value to such assumptions. For layers with low concentration of conodonts such as these calciturbidites, each sample (to be considered in the future) should be over 10 kg.

The relatively small thickness of the *kockelianus* and *eiflius* (if present) zones in the PE-C section suggest a lower carbonate sedimentation rate for this particular interval of approximately a million years, given the latest estimates for the Eifelian age (Fig. 5).

6.2 Paleoenvironment and geodynamic considerations

In the Odivelas Limestone (SW boundary of OMZ, located to the south of PE quarry; Fig. 1a), there are two calciturbidite sequences, which were previously sampled for conodonts: Covas Ruivas section, which yielded conodonts from the *patulus* (uppermost Emsian) to *australis* zones (lowermost zone of the upper part of the Eifelian) (Machado et al., 2010); and Cortes section, yielding conodonts from

the *hemiansatus* zone (lowermost Givetian) (Machado et al., 2020a) (Fig. 5). In the Cortes section, crinoids, tabulate and rugose corals, and stromatoporoids indicate a reef structure ranging between late Eifelian to early Givetian age (Fig. 5; Machado et al., 2009). The Odivelas Limestone sections show the relation between the reefal and calciturbidite facies, which are interpreted as belonging to a series of atoll-like reef structures developed along the SW boundary of the OMZ (Machado et al., 2020b; Moreira et al., 2021; Oliveira et al., 2019), here associated with volcanic activity (Moreira et al., 2010; Oliveira et al., 2019). The dominance of fine-grained calciturbidites in the PE Limestone seems to record a distal depositional environment (possibly the base of a slope) of low-density carbonate turbidites deriving from a reef area, suggesting a possible relation between the depositional environment of Pedreira de Engenharia calciturbidites and those described for the Odivelas Limestone. The presence of crinoid fragments, mainly in the basal part of the succession, together with significant amounts of dacryconarids in the upper part of the succession, also indicate a more distal depositional environment. In the case of the PE Limestone, evidence of synchronous volcanic activity is absent, indicating that reef-like structures developed over previously deformed basement highs of OMZ lower Paleozoic successions (in accordance with the proposal of Oliveira et al., 2019). Consequently, the Devonian carbonate sedimentation along the SW border of the OMZ (composed of Odivelas, Atalaia, Pena, Caeirinha and Pedreira de Engenharia limestones; see Fig. 1) can be interpreted as peri-reefal calciturbidites, associated to a reefal system, which is only preserved in the Cortes section (Fig. 5).

The atoll-like structures developed at shallow depth for the colonization and development of reef building taxa to occur. These environmental conditions allowed the erosion/dismantlement of reef systems, developed on the flanks of the volcanic edifices (case of Odivelas Limestone) or on/over basement highs (case of Pedreira de Engenharia Limestone), generating coeval peri-reefal sedimentation represented by the calciturbidite successions, which extend at least to the base of the slope, similar to those described in other places in the north Gondwana realm (e.g. Denayer, 2023; Galle et al., 1995; Jakubowicz et al., 2018; Suttner et al., 2021).

Concerning the diagenetic and tectonic history of the PE Limestone, the following facts should be taken into consideration:

- CAI value of the conodont elements (5 to 5.5) is indicative of a high peak temperature, likely exceeding the 300 °C (Epstein et al., 1977);
- The metamorphism and deformation of the PE Limestone contrasts with those affecting the Cabrela (very low grade and only affected by slaty cleavage) and Carvalhal formations (greenschist to amphibolite facies) (Chichorro et al.,

2008; Oliveira et al., 1991, 2019; Pereira et al., 2006; Theias et al., 2018);

- Although not recognized during the recent fieldwork, a conglomerate layer has been described at the base of the PE Limestone, overlying the Carvalhal Formation, and another conglomerate layer (this one observed in the field) is found at the lowermost levels of the Cabrela Formation (Oliveira et al., 1991; Ribeiro, 1983).

Considering the above, the relation between the PE Limestone with both the Cabrela and Carvalhal formations comes down to two hypotheses:

- Hypothesis 1 (discussed by Oliveira et al., 2019): The Cabrela Formation overlies the PE Limestone. The Cambrian Carvalhal Formation was probably deformed during the early stages of the Devonian subduction process of the South Portuguese Terrain underneath the Gondwana continent (OMZ in this case; Oliveira et al., 2019). After the deposition of the PE Limestone, in the Middle Devonian, both the PE Limestone and Carvalhal Formation experienced an identical burial history, being heated and deformed during the subduction process to temperatures exceeding 300°C. After this, during the early Carboniferous, the exhumation of autochthonous units (including Carvalhal Formation and PE Limestone) was followed by deposition of the Cabrela Formation, and both contributed to the sedimentation of the siliciclastic turbidites of this unit. This is in accordance with the presence of phyllites and greenschists in the basal conglomerate of the Cabrela Formation and some limestone boulders within the southern edges of the Cabrela Basin (Machado et al., 2022; Oliveira et al., 1991; Pereira et al., 2006). The discrepant geometric features of deformation between Cabrela Formation and the PE limestones also indicate distinct tectonometamorphic evolution of the two units.
- Hypothesis 2 (suggested by Pereira & Oliveira, 2003): The PE Limestone is an olistolith within the Mississippian Cabrela Basin. In this hypothesis, the conglomerate layer at its base is the result of the sliding motion of the limestone body on the ocean floor, at the beginning of the filling of the Cabrela Basin, partially eroding the underlying Carvalhal Formation. If the transport of the PE limestone occurred sometime during an advanced stage of filling of the basin, then it would likely be overlying the Cabrela Formation. For the olistolith hypothesis to be plausible, the transport should have occurred at an early stage of basin filling, assuming there is a conglomerate layer at the base of the PE Limestone and that it overlies the Carvalhal Formation—as mentioned, neither observation could be confirmed during field work. Furthermore, the general geometry of the PE Limestone is in

accordance with the regional model of deformation, and not inverted, rotated or chaotic. To validate this hypothesis, the limestone boulder must have slid down the slope while maintaining its attitude. The conglomerate at the base of the limestone body may also be the product of early sedimentation under slope conditions, with higher energy and coarser sediment. Both hypotheses can also explain the presence of the younger Frasnian limestone boulders within the Cabrela Formation (Boogaard, 1983; Oliveira et al., 2019).

Regardless of the hypothesis, the carbonate sedimentation during Early to Middle Devonian (uppermost Emsian until lowermost Givetian) in the SW branch of OMZ agrees with the general geodynamic model of the Iberian Variscides. Indeed, several authors point to the beginning of the subduction of the Variscan Ocean(s) along the northern margin of Gondwana (including the OMZ) during the Early Devonian (e.g., Dias et al., 2016; Moreira et al., 2014; Oliveira et al., 2019; Pereira et al., 2012; Ribeiro et al., 2007). The paleogeographic context of the northern realm of Gondwana, during this geological period, is characterized by extensive epicontinental seas, developed in low to mid latitudes and associated with paleoclimatic conditions (e.g., Bábek et al., 2018; Becker et al., 2020) that enhanced the biological productivity and carbonate sedimentation. In the SW branch of the Iberian Massif, namely in the SW of the OMZ, the subduction processes generated a volcanic arc and seafloor elevations (basement highs) during the early deformation episodes. Thus, this local paleogeographic setting and the paleoclimatic conditions may have favored the development of reef fauna, with generation of atoll-like structures, and associated calciturbidite successions. The crustal uplift of the southernmost Iberian Massif during the Middle Devonian (Moreira et al., 2014; Oliveira et al., 2019) explains the general absence of sedimentation in most of the OMZ (e.g., Robardet & Gutiérrez-Marco, 2004). Exceptions are found in the SW branch of the OMZ, where the Odivelas and Pedreira de Engenharia limestones were deposited, probably representing isolated reef-like structures, not larger than a few km across, and so explaining their scarce and isolated nature.

7 Conclusions

Fifteen conodont species, belonging to *Icriodus*, *Polygnathus* and *Tortodus*, were identified, ranging from the *costatus* (lower Eifelian) to the *ensensis* zones (uppermost Eifelian). The Pedreira da Engenharia Limestone quarry section was subdivided into three subsections, all around 14 m thick: PE-A, dating from the lower Eifelian (no specified biozones); PE-B, dating from the *costatus* to the *australis*

zones; and PE-C, ranging from the *costatus* to the *ensensis* zones. The CAI value of 5 to 5,5 of the conodont elements indicates a maximum temperature of over 300 °C. The *kockelianus* and *eiflius* zones appear to be condensed to 1,5 m of succession, indicating a lower carbonate sedimentation rate during this time. The PE Limestone is quite similar to the Odivelas Limestone (further south) in age, lithology and depositional setting, which indicates a possible connection between the two units. Both the Odivelas and PE Limestone evidence the development of calciturbidite sedimentation associated with atoll-like structures (only preserved in Odivelas) along the SW margin of the OMZ, being probably associated with the beginning of the subduction process of the Rheic Ocean during Early to Middle Devonian times.

Acknowledgements The authors thank Stana Vodrážková and Sören Jensen for the revision of the manuscript, to João Cascalho and Pedro Costa for the bromoform made available for this project and to Ms. Maria da Paz for the access to the quarry area. JCL is supported by Maria Zambrano Grant (MIU Next Generation EU, ZA21-005 and José Castillejo Fellowship (MICCIN-MIU, CAS22/00148). GS is funded through a PhD grant from Fundação para a Ciência e Tecnologia (ref. 2020.08450.BD). The project ALT20-03-0145-FEER-000028, co-financed by Alentejo 2020 through FEDER/FSE/FEEI, financed the field work. GS and NM are supported by national funding awarded by FCT—Foundation for Science and Technology, I.P., projects UIDB/04683/2020 and UIDP/04683/2020. This work represents a contribution to the UNESCO-IGCP 652 project: “Reading geologic time in Palaeozoic sedimentary rocks”, and to the research groups PALPAL (GIUV2017-395) and PERIGONDWANA (UCM 910231).

Funding Open access funding provided by FCTIFCCN (b-on).

Data availability The authors confirm that the data supporting the findings of this study are available within the article.

Declarations

Conflict of interest On behalf of all authors, the corresponding author states that there is no conflict of interest.

Open Access This article is licensed under a Creative Commons Attribution 4.0 International License, which permits use, sharing, adaptation, distribution and reproduction in any medium or format, as long as you give appropriate credit to the original author(s) and the source, provide a link to the Creative Commons licence, and indicate if changes were made. The images or other third party material in this article are included in the article’s Creative Commons licence, unless indicated otherwise in a credit line to the material. If material is not included in the article’s Creative Commons licence and your intended use is not permitted by statutory regulation or exceeds the permitted use, you will need to obtain permission directly from the copyright holder. To view a copy of this licence, visit <http://creativecommons.org/licenses/by/4.0/>.

References

- Andrade, A., Pinto, A., & Conde, L. (1976). Sur la géologie du Massif de Beja: Observations sur la transversale d’Odivelas. *Comunicações Dos Serviços Geológicos De Portugal*, 60, 171–202.

- Bábek, O., Faměra, M., Šimíček, D., Weinerová, H., Hladil, J., & Kalvoda, J. (2018). Sea-level changes vs. organic productivity as controls on Early and Middle Devonian bioevents: Facies- and gamma-ray based sequence-stratigraphic correlation of the Prague Basin, Czech Republic. *Global and Planetary Change*, 160(2018), 75–95. <https://doi.org/10.1016/j.gloplacha.2017.11.009>
- Bardashev, I. A. (1991). Stratigraphy and conodonts of the Eifelian deposits of Central Tajikistan. In: Khalym-Badzha, V. J. (Ed.), *Conodonts of the USSR Eifelian Stage*, Kazan, 25–41.
- Bardashev, I. A. (1992). Conodont stratigraphy of middle Asian Middle Devonian. *Courier Forschungsinstitut Senckenberg*, 154, 31–83.
- Bardashev, I. A., & Ziegler, W. (1985). Conodonts from a Middle Devonian section in Tadzhikistan (Kalagach Fm., Middle Asia, USSR). *Courier Forschungsinstitut Senckenberg*, 75, 65–78.
- Becker, R. T., Aboussalam, Z. S. (2013). The global Chotec Event at Jebel Amelane (western Tafilalt Platform) – preliminary data. In: Becker R, El Hassani A, Tahiri A (Eds), International Field Symposium “The Devonian and Lower Carboniferous of northern Gondwana”, Field Guidebook, Document de l’Institut Scientifique, Rabat, 27, 129–134.
- Becker, R. T., Marshall, J. E. A., Da Silva, A.-C. (2020). The Devonian Period. *Geologic Time Scale 2020*. <https://doi.org/10.1016/B978-0-12-824360-2.00022-X>
- Belka, Z., Kaufmann, B., & Bultynck, P. (1997). Conodont-based quantitative biostratigraphy for the Eifelian of the eastern Anti-Atlas, Morocco. *GSA Bulletin*, 109(6), 643–651.
- Berkyová, S. (2009). Lower-Middle Devonian (upper Emsian-Eifelian, serotinus-kockelianus zones) conodont faunas from the Prague Basin, the Czech Republic. *Bulletin of Geosciences*, 84(4), 667–686. <https://doi.org/10.3140/bull.geosci.1153>
- Bischoff, G., Ziegler, W. (1957). Die Conodontenchronologie des Mitteldevons und des tiefsten Oberdevons. *Abhandlungen des Hessischen Landesamtes für Bodenforschung*, 22, 136 pp.
- Branson, E. B., Mehl, M. G. (1933). Conodont studies, No. 1, 2. *University of Missouri Studies*, 8.
- Bultynck, P. (1970). Révision stratigraphique et paléontologique de la coupe type du Couvinien. *Mémoires de l’Institut Géologique de l’Université de Louvain*, 26, 152 pp.
- Bultynck, P. (1987). Pélagic and neritic conodont successions from the Givetian of pre-Sahara Morocco and the Ardennes. *Sciences De La Terre*, 57, 149–181.
- Bultynck, P. (2006). Couvinien. *Geologica Belgica*, 9(1/2), 147–150.
- Carvalhosa, A., Zbyszewski, G. (1994). Carta Geológica de Portugal, na escala 1:50 000 e Notícia Explicativa - folha 35-D (Montemor-o-Novo). Serviços Geológicos de Portugal, 87 pp.
- Chichorro, M. (2006). Estrutura do Sudoeste da Zona de Ossa-Morena: Área de Santiago de Escoural—Cabrela (Zona de Cisalhamento de Montemor-o-Novo, Maciço de Évora). Ph.D. thesis (unpublished), Universidade de Évora, Portugal, 502 pp.
- Chichorro, M., Pereira, M., Díaz-Azpiroz, M., Williams, I., Fernández, C., Pin, C., & Silva, J. (2008). Cambrian ensialic rift-related magmatism in the Ossa-Morena Zone (Évora–Aracena metamorphic belt, SW Iberian Massif): Sm–Nd isotopes and SHRIMP zircon U–Th–Pb geochronology. *Tectonophysics*, 461, 91–113.
- Cohen, K. M., Finney, S. C., Gibbard, P. L., Fan, J.-X. (2023). International Chronostratigraphic Chart. International Commission on Stratigraphy (available at <https://stratigraphy.org/>, consulted at 1st February 2023).
- Denayer, J. (2023). From mud to limestone: Birth and growth of a giant reef in the Eifelian (Middle Devonian) of S Belgium. *Palaeogeography, Palaeoclimatology, Palaeoecology*, 627, 111748. <https://doi.org/10.1016/j.palaeo.2023.111748>
- Dias, R., Ribeiro, A., Romão, J., Coke, C., & Moreira, N. (2016). A review of the Arcuate Structures in the Iberian Variscides; Constraints and Genetic Models. *Tectonophysics*, 681C, 170–194. <https://doi.org/10.1016/j.tecto.2016.04.011>
- Epstein, A. G., Epstein, J. B., & Harris, L. D. (1977). Conodont color alteration—An index to organic metamorphism. *Geological Survey Professional Paper*, 995, 1–27.
- Galle, A., Hladil, J., & Isaacson, P. E. (1995). Middle Devonian Biogeography of Closing South Laurussia–North Gondwana Variscides: Examples from the Bohemian Massif (Czech Republic), with Emphasis on Horní Benešov. *Palaios*, 10(3), 221–239.
- Hinde, G. J. (1879). On Conodonts from the Chazy and Cincinnati Group of the Cambro-Silurian, and from the Hamilton and Genesee-Shale Divisions of the Devonian, in Canada and the United States. *Quarterly Journal of the Geological Society*, 139, 351–369.
- Jakubowicz, M., Król, J., Zapalski, M. K., Wrzolek, T., Wolniewicz, P., & Berkowski, B. (2018). At the southern limits of the Devonian reef zone: Palaeoecology of the Aferdou el Mrakib reef (Givetian, eastern Anti-Atlas, Morocco). *Geological Journal*. <https://doi.org/10.1002/gj.3152>
- Jorge, J., Machado, G., Moreira, N., Silvério, G., Ramos, M., Esteves, C., Theias, A., & Cachão, M. (2018). Petrografia dos Calcários Devonianos da Formação Pedreira da Engenharia, W da Zona de Ossa-Morena, Portugal. *Livro De Actas Do VIII Congresso Jovens Investigadores Em Geociências, LEG, 2018*, 102–105.
- Klapper, G. (1971). Sequence within the conodont genus *Polygnathus* in the New York lower Middle Devonian. *Geologica Et Palaeontologica*, 5, 59–79.
- Klapper, G., Ziegler, W., & Mashkova, T. V. (1978). Conodonts and correlation of Lower-Middle Devonian boundary beds in the Barrandian area of Czechoslovakia. *Geologica Et Palaeontologica*, 12, 103–116.
- Koptíková, L. (2011). Precise position of the Basal Chotec event and evolution of sedimentary environments near the Lower-Middle Devonian boundary: The magnetic susceptibility, gamma-ray spectrometric, lithological, and geochemical record of the Prague Synform (Czech Republic). *Palaeogeography, Palaeoclimatology, Palaeoecology*, 304(1–2), 96–112. <https://doi.org/10.1016/j.palaeo.2010.10.011>
- Liao, J.-C., & Valenzuela-Ríos, J. I. (2008). Givetian and early Frasnian conodonts from the Compte section (Middle-Upper Devonian, Spanish Central Pyrenees). *Geological Quarterly*, 52(1), 1–18.
- Liao, J.-C., & Valenzuela-Ríos, J. I. (2013). The Middle and Upper Devonian conodont sequence from La Guardia D’Àres Sections (Spanish Central Pyrenees). *Bulletin of Geosciences*, 88(2), 339–368.
- Machado, G., Hladil, J. (2010). On the age and significance of the limestone localities included in the Toca da Moura volcano-sedimentary Complex: preliminary results. In: Santos, A., Mayoral, E., Melendez, G., Silva, C.M.D., Cachão, M. (Ed.), III Congresso Iberico de Paleontologia / XXVI Jornadas de la Sociedad Espanola de Paleontologia, Lisbon, Portugal. *Publicaciones del Seminario de Paleontologia de Zaragoza (PSPZ)*, 9, 153–156.
- Machado, G., Moreira, N., Neto De Carvalho, C., Madrinha, J., Esteves, C. J. P., Kalvoda, J., Theias, A., Jorge, J., Ramos, M., Silva, B., Sousa, D., Caralinda, I., Cachão, M. (2022). The Mississippian Toca da Moura-Cabrela Basin (SW Ossa-Morena Zone, Portugal): sedimentation and palaeoenvironments. International meeting: Ossa Morena and beyond; a tribute to Teodoro Palacios, Universidade da Extremadura, Badajoz, 25–26.
- Machado, G., Hladil, J., Koptikova, L., Fonseca, P., Rocha, F. T., & Galle, A. (2009). The Odivelas Limestone: Evidence for a Middle Devonian reef system in western Ossa-Morena Zone. *Geologica Carpathica*, 60(2), 121–137.
- Machado, G., Hladil, J., Koptikova, L., Slavik, L., Moreira, N., Fonseca, M., & Fonseca, P. (2010). An Emsian-Eifelian Carbonate-Volcaniclastic Sequence and the possible Record of the basal chotec event in western Ossa-Morena Zone, Portugal (Odivelas Limestone). *Geologica Belgica*, 13, 431–446.

- Machado, G., Moreira, N., & Silvério, G. (2020b). Devonian sedimentation in the SW boundary of the Ossa-Morena Zone; State of Art and Paleogeography. *Comunicações Geológicas*, 107, 43–47.
- Machado, G., Slavik, L., Moreira, N., & Fonseca, P. E. (2020a). Prasinophyte bloom and putative fungi abundance near the Kačák event (Middle Devonian) from the Odívelas Limestone, Southwest Iberia. *Palaeobiodiversity and Palaeoenvironments*, 100, 593–603. <https://doi.org/10.1007/s12549-019-00415-1>
- Moreira, N., Araújo, A., Pedro, J. C., & Dias, R. (2014). Evolução geodinâmica da Zona de Ossa-Morena no contexto do SW Ibérico durante o Ciclo Varisco. *Comunicações Geológicas*, 101(Vol. Especial I), 275–278.
- Moreira, N., Machado, G., Fonseca, P. E., Silva, J. C., Jorge, R. C. G. S., & Mata, J. (2010). The Odívelas Palaeozoic volcano-sedimentary sequence; implications on the Ossa-Morena SW border. *Comunicações Geológicas*, 97, 129–146.
- Moreira, N., Machado, G., & Silvério, G. (2021). Lower-Middle Devonian limestones of the SW border of the Ossa-Morena Zone; from local to global paleogeographic scale. *Geo-Temas*, 18, 1079–1083.
- Moreira, N., Pedro, J., Santos, J. F., Araújo, A., Dias, R., Ribeiro, S., Romão, J., & Mirão, J. (2019). 87Sr/86Sr applied to age discrimination of the Palaeozoic carbonates of the Ossa-Morena Zone (SW Iberia Variscides). *International Journal of Earth Sciences (geol Rundsch)*, 108(3), 963–987. <https://doi.org/10.1007/s00531-019-01688-9>
- Oliveira, J. T., Relvas, J., Pereira, Z., Munhá, J., Matos, J., Barriga, F., Rosa, C. (2013). O Complexo Vulcano-Sedimentar de Toca da Moura-Cabrela (Zona de Ossa Morena): evolução tectono-estratigráfica e mineralizações associadas. In: Dias R, Araújo A, Terrinha P, Kullberg JC (Ed), *Geologia de Portugal (Vol. I)*, Escolar Editora, Lisboa, 621–645.
- Oliveira, J. T., González-Clavijo, E., Alonso, J., Armendáriz, M., Bahamonde, J. R., Braid, J. A., Colmenero, J. R., Dias Da Silva, I., Fernandes, P., Fernández, L. P., Gabaldón, V., Jorge, R. S., Machado, G., Marcos, A., Merino-Tomé, Ó, Moreira, N., Brendan Murphy, J., Pinto De Jesus, A., Quesada, C., Rodrigues, B., Rosales, I., Sanz-López, J., Suárez, A., Villa, E., Piçarra, J.M., Pereira, Z. (2019). Synorogenic Basins. In: QUESADA, C., OLIVEIRA, J. T. (Eds.), *The Geology of Iberia: a geodynamic approach (Volume 2: The Variscan Cycle)*. Springer (Berlin), Regional Geology Review series, 349–429 https://doi.org/10.1007/978-3-030-10519-8_11
- Oliveira, J., Oliveira, V., & Piçarra, J. (1991). Traços gerais da evolução tectono-estratigráfica da Zona de Ossa-Morena, em Portugal. *Comunicações Dos Serviços Geológicos De Portugal*, 77, 3–26.
- Pander, C. H. (1856). Monographie der fossilen Fische des silurischen Systems des russisch-baltischen Gouvernements. *Buchdruckerei der Kaiserlichen Akademie der Wissenschaften*, 1, 1–91.
- Pedder, A. E., Jackson, J. H., & Philip, G. M. (1970). Lower Devonian biostratigraphy in the Wee Jasper region of new South Wales. *Journal of Paleontology*, 44(2), 206–251.
- Pereira, M. F., Chichorro, M., Johnston, S. T., Gutiérrez-Alonso, G., Silva, J. B., Linnemann, U., Hofmann, M., & Drost, K. (2012). The missing Rheic Ocean magmatic arcs: Provenance analysis of Late Paleozoic sedimentary clastic rocks of SW Iberia. *Gondwana Research*, 22, 882–891. <https://doi.org/10.1016/j.gr.2012.03.010>
- Pereira, Z., & Oliveira, J. T. (2003). Estudo palinostratigráfico do sinclinal da Estação de Cabrela. *Implicações Tectonostratigráficas. Ciências Da Terra UNL*, 5, 118–119.
- Pereira, Z., Oliveira, V., & Oliveira, J. T. (2006). Palynostratigraphy of the Toca da Moura and Cabrela Complexes, Ossa Morena Zone, Portugal. Geodynamic implications. *Review of Palaeobotany and Palynology*, 139, 227–240.
- Piçarra, J. M., & Sarmiento, G. (2006). Problemas de posicionamento estratigráfico dos Calcários Paleozóicos da Zona de Ossa Morena (Portugal). *Abstracts of the VII Congresso Nacional De Geologia, Estremoz, II*, 657–660.
- Ribeiro, A. (1983). Relações entre formações do Devónico superior e o Maciço de Évora na região de Cabrela (Vendas Novas). Guia das excursões no bordo sudoeste da Zona de Ossa-Morena. *Comunicações Dos Serviços Geológicos De Portugal*, 69(2), 267–282.
- Ribeiro, A., Munhá, J., Dias, R., Mateus, A., Pereira, E., Ribeiro, L., Fonseca, P., Araújo, A., Oliveira, T., Romão, J., Chaminé, H., Coke, C., & Pedro, J. (2007). Geodynamic evolution of the SW Europe Variscides. *Tectonics*, 26(6), 24. <https://doi.org/10.1029/2006TC002058>
- Robardet, M., & Gutiérrez-Marco, J. C. (2004). The Ordovician, Silurian and Devonian sedimentary rocks of the Ossa-Morena Zone (SW Iberian Peninsula, Spain). *Journal of Iberian Geology*, 30, 73–92.
- Santos, J. F., Andrade, A., & Munhá, J. (1990). Magmatismo orogénico varisco no limite meridional da Zona de Ossa-Morena. *Comunicações Dos Serviços Geológicos De Portugal*, 76, 91–124.
- Sarmiento, G. N., Piçarra, J. M., Oliveira, J. T. (2000). Conodontes do Silúrico (Superior?)–Devónico nos “Mármore de Estremoz”, Sector de Estremoz-Barrancos (Zona de Ossa Morena, Portugal). Implicações estratigráficas e estruturais a nível regional. *I Congresso Ibérico de Paleontologia/VIII International Meeting of IGCP 421 (abstract book)*, Évora, 284–285.
- Sarmiento, G. N., Gutiérrez-Marco, J. C., Rodríguez-Cañero, R., Martín-Algarra, A., Navas-Parejo, P. (2011). A brief summary of Ordovician Conodont Faunas from the Iberian Peninsula. In: Gutiérrez-Marco JC, Rábano I, García-Bellido D (eds) *Ordovician of the World. Cuadernos del Museo Geominero IGME*, 14, 505–514.
- Sarmiento, G. N., Gutiérrez-Marco, J. C., & Del Moral, B. (2008). Conodontes de la “Caliza de Pelmatozoos” (Ordovícico Superior), Norte de Sevilla, Zona de Ossa-Morena (España). *Coloquios De Paleontologia*, 58, 73–99.
- Suttner, T. J., Kido, E., Joachimski, M. M., Vodrážková, S., Pondrelli, M., Corradini, C., Corrigan, M. G., Simonetto, L., & Kubajko, M. (2021). Paleotemperature record of the Middle Devonian Kačák Episode. *Scientific Reports*, 11, 16559. <https://doi.org/10.1038/s41598-021-96013-3>
- Theias, A., Moreira, N., Machado, G., Ramos, M., Silvério, G., Jorge, J., Esteves, C., & Cachão, M. (2018). Estrutura dos Calcários da Pedreira da Engenharia e a sedimentação carbónica envolvente: Implicações geodinâmicas. *Livro De Actas Do VIII Congresso Jovens Investigadores Em Geociências, LEG, 2018*, 94–97.
- van den Boogaard, M. (1972). Conodont faunas from Portugal and southwestern Spain. Part 1. A Middle Devonian fauna from near Montemor-o-Novo. *Scripta Geologica*, 13, 1–11.
- van den Boogaard, M. (1983). Conodont faunas from Portugal and southwestern Spain. Part 7. A Frasnian conodont fauna near the Estação de Cabrela (Portugal). *Scripta Geologica*, 69, 1–17.
- Vodrážková, S., Frýda, J., Suttner, T. J., Koptíková, L., & Tonarová, P. (2012). Environmental changes close to the Lower-Middle Devonian boundary; the Basal Chotec Event in the Prague Basin (Czech Republic). *Facies*, 59, 425–449. <https://doi.org/10.1007/s10347-012-0300-x>
- Vodrážková, S., Klapper, G., & Murphy, M. A. (2011). Early Middle Devonian conodont faunas (Eifelian, *costatus*–*kockelianus* zones) from the Roberts Mountains and adjacent areas in central Nevada. *Bulletin of Geosciences*, 86(4), 737–764.
- Walliser, O., & Bultynck, P. (2011). Extinctions, survival and innovations of conodont species during the Kačák Episode (Eifelian-Givetian) in south-eastern Morocco. *Sciences De La Terre*, 81, 5–25.
- Weddige, K. (1977). Die conodonten der Eifel-Stufe im Typusgebiet und in benachbarten Faziesgebieten. *Senckenbergiana Lethaea*, 58(4/5), 271–419.

- Wittekindt, H. (1965). C. Probleme der stratigraphischen Grenzen. Zur conodontenchronologie des Mittledevons. *Fortschritte in der Geologie Von Rheinland und Westfalen*, 9, 621–645.
- Ziegler, W., Klapper, G., & Johnson, J. G. (1976). Redefinition and subdivision of the *varcus*-Zone (Conodonts, Middle-?Upper

Devonian) in Europe and North America. *Geologica Et Palaeontologica*, 10, 109–140.